ISSN: 2755-984X

Journal of Tumor Science Research

SCIENTIFIC Research and Community

Research Article

Open Access

Simulating the Role of RAD51 Over-Expression on DNA Repair and its Potential Impact on Tumor Prognosis via Targeted Gene Therapy

Adhith Theyver[1]* and Ngan Phan[2]

[1]West Ranch High School, Stevenson Ranch, CA, USA

[2]Kennesaw State, University Marietta, USA

ABSTRACT

ROS-induced DNA damage is particularly detrimental in the context of cancers as it oxidatively stresses the tumor microenvironment (TME). Cells in the TME play a vital role in cancer pathogenesis, and by understanding the therapeutic strategies, ROS-induced damage can be mitigated. ROS causes single-strand DNA breaks (SSBs) and double-strand breaks (DSBs), and the accumulation of these breaks leads to genomic instability and cancer progression. This study focuses on the pathway and effects of introducing DNA repair proteins (RAD51 in this study) via adenoviral vectors into the TME to reduce ROS-induced DNA damage. RAD51 is a repair protein involved in homologous recombination to anneal DSBs. Adenoviruses are double-stranded DNA viruses ubiquitous in common diseases; however, their DNA sequence/plasmid is commonly used in clinical gene therapies as a medium of gene insertion. This study simulates various laboratory techniques necessary for adenoviral generation.

After insertion, the effects of RAD51 are theorized in a Western Blot measuring phosphorylated H2AX (γH2AX). γH2AX can be used as a biomarker for RAD51, as it plays a vital role in accumulating DNA repair proteins at the site of the break: when there are more breaks, there will be a larger concentration of γH2AX. This study is a gene therapy methodology that simulates adenoviral generation, focusing on the engineered vector designed for therapy. If future preclinical studies validate this research, it could lead to significant benefits for patients, such as reducing their resistance to radiotherapy and decreasing overall malignancy.

***Corresponding author**

Adhith Theyver, West Ranch High School, Stevenson Ranch, CA, USA.

Received: September 16, 2025; **Accepted:** September 20, 2025; **Published:** September 30, 2025

Keywords: ROS, Tumor Microenvironment, DNA Repair Proteins, Rad51, γh2ax, Adenoviral Vectors

Introduction

This paper aims to explore gene therapy's impact on the prognosis of ROS-related tumors by enhancing DNA repair proteins within the TME. Given that ROS can induce DNA damage, this aims to determine whether increasing the expression of DNA repair proteins through targeted gene therapy can improve treatment outcomes [1]. Part of the study was simulated using SnapGene, and the remainder was completed by following Addgene and SnapGene protocols as guidelines [2-9].

ROS

Reactive Oxygen Species (ROS) are highly reactive chemicals formed from diatomic oxygen, water, and hydrogen peroxide; ROS are formed in all cells as a byproduct of cellular respiration [10,11].

ROS in Cancer

Tumor cells and unaffected somatic cells produce ROS [12-13]. However, the rate of ROS production is significantly elevated in tumor cells because tumor cells have an increased metabolic rate and exist in hypoxia. Tumors carry out the increased metabolism via the Warburg Effect: a phenomenon where cancer cells produce energy from glycolysis and lactic acid fermentation [14]. Hypoxia affects the cells' oxygen-reliant pathways as the electron transport chain is disrupted when there is limited oxygen [15]. Without the final electron acceptor, built-up electrons partially reduce oxygen molecules and produce ROS.

ROS Damage to DNA

The resulting increase in ROS can be particularly detrimental to DNA by inducing DNA single- strand breaks (SSBs). One way this occurs is the production of an oxidative lesion (8-oxo-guanine or 8- oxoG) or a thymine glycol [16]. Oxidative lesions occur when hydroxyl radicals oxidize the respective base. When DNA polymerase encounters an oxidative lesion, it may mistakenly add an adenine opposite to the 8-oxoG. During base excision repair (BER), the AP endonuclease protein improperly nicks the DNA to remove the 8-oxoG, which results in a single-strand break (SSB); an accumulation of SSBs will lead to DNA double-stranded breaks (DSBs). If thymine glycol lesions occur–when thymine derivatives have unorthodox binding with their adenine counterparts–then DNA polymerase will be stalled at the replication fork, which can lead to SSBs or DSBs [17-18].

ROS Affecting the Tumor Microenvironment

ROS significantly impacts the tumor microenvironment (TME) by promoting genetic instability, altering cellular behavior, and supporting tumor progression and metastasis through its effects on -,n nn n n, n fibroblasts and immune cells. Cancer-associated fibroblasts (CAFs) are key players in cancer initiation, progression, and metastasis, especially when they are on the tumor periphery [19-21].

ROS influences the differentiation of stem cells into CAFs in various ways. For example, ROS enhances the expression of cytokine TGF-β by increasing the activation of TGF-β ligands and receptors [22]. Furthermore, ROS has been shown to inhibit phosphatases that normally suppress TGF-β signaling, resulting in prolonged activation of the TGF-β pathway. Increased activation and prolongation of the TGF-β pathway lead to an increase in CAFs within the tumor microenvironment. Weinberg et. al. co-cultured breast cancer cells with CAFs to show the effects of hydrogen peroxide (ROS) on CAFs [23].

Their results showed CAV-1 downregulation and increased expression of myofibroblast biomarkers.

CAV-1 is a tumor suppressor protein, and its downregulation yields further tumorigenesis [24]. In their conclusion, they stated ROS could alter the CAF phenotype to create a tumorigenic microenvironment.

CAFs affect the DNA of cells in the TME by secreting growth factors (EGF and HGF), cytokines (e.g., IL-6, IL-8), chemokines, and ROS [25]. These secretions can induce DNA damage and promote genomic instability in nearby cells. For example, both EGF and IL-8 transactivation result in increased levels of intracellular ROS [26-29]. An increased concentration of ROS leads to further differentiation of CAFs and, inadvertently, tumorigenesis.

Tumor-originating ROS can impact the TME both directly, by spreading into the surrounding environment, and indirectly, through extracellular vesicles (EVs) [23,30]. As mentioned previously, CAV-1 downregulation is a notable characteristic of many ROS-associated cancers; CAV-1 downregulation leads to increased exosomal uptake of stromal cells. Paggetti et. al. demonstrated that chronic lymphocytic leukemia-derived (CLL) exosomes caused stromal cells in the TME to exhibit phenotypic properties characteristic of CAFs [31]. The affected stromal cells exhibited increased proliferation, migration, and secretion of tumor-supportive cytokines, leading to tumor progression. Since ROS enhances exosomal uptake, it ultimately increases the number of stromal cells adopting the CAF phenotype, supporting tumor growth.

Approach

If we limit the ROS damage to the DNA of cells in the TME, we can prevent the excessive proliferation of CAFs. A lower amount of CAFs would result in fewer tumorigenic secretions, leading to a slower rate of carcinogenesis. Also, limiting ROS damage can prevent the overexpression of CAFs by reducing exosomal uptake. Thus, this study designs and outlines a gene therapy approach that uses adenoviral vectors with RAD51, a DNA repair protein. The study uses the molecular cloning method to generate an ideal adenoviral vector from the pAMHDAdGT8-4 adenoviral plasmid. RAD51–a DNA repair protein that anneals DSBs–is the gene proposed for insertion into the designed adenoviral plasmid. RAD51 may improve the efficacy of existing cancer therapies by hindering tumor progression.

Data

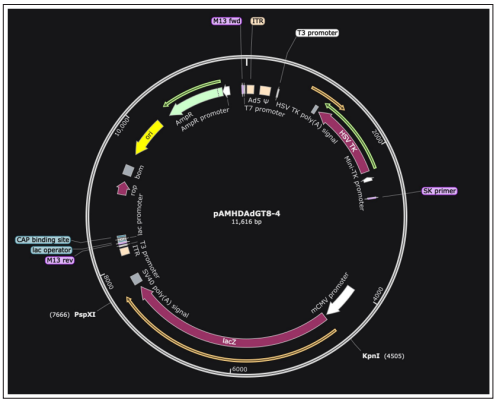

Figure 1: Pamhdadgt8-4 Gene Sequence

PspXI (Restriction Site on Nucleotide Position 7666) and KpnI (Restriction Site on Nucleotide Position 4505) are the Restriction Enzymes Marked. [Graph Created by The Student Researcher using SnapGene, 2024]

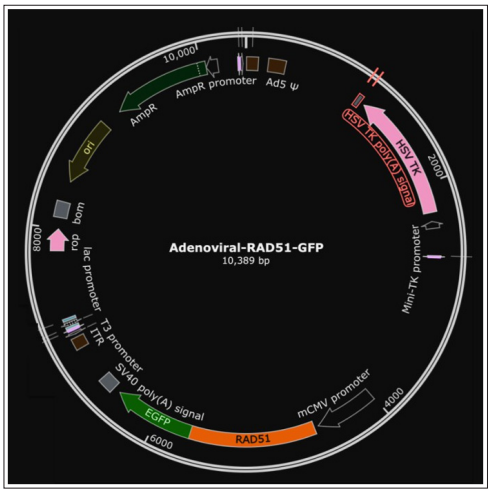

Figure 2: Adenoviral-Rad51-Egfp Plasmid After Pamhdadgt8-4 Digestion Reaction

eGFP (Green) and RAD51 (Orange) were Inserted into the Location of the lacZ gene, between the SV40 poly (A) Signal and Mcmv Promoter. [Image Created by Student Using Snapgene During Digestion Reaction, 2024]

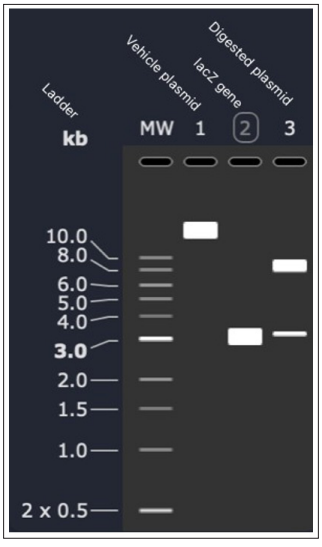

Figure 3: Electrophoresis Simulation Results

The agarose gel's result **Simulation Ran on SnapGene**. The schematic for the electrophoresis reaction was run to measure the accuracy of the digestion reaction. A 1kb DNA ladder was added to the unmarked lane; lane 1 contains the undigested pAMHDAdGT8-4 plasmid; lane 2 contains only the lacZ gene fragment; and lane 3 has the KpNI and PsPXI digested pAMHDAdGT8-4. [Graph created by the student researcher using SnapGene electrophoresis simulation, 2024]

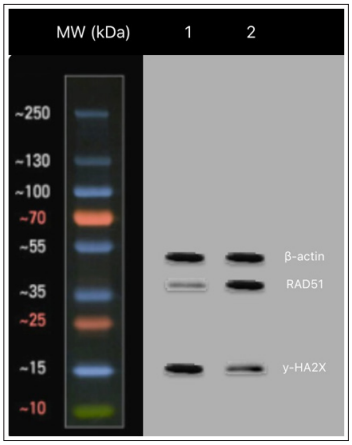

Figure 4: Predicted Western Blot

The 1kb plus DNA ladder (NEB #N3200S) was used as a standard for protein molecule weight (in kDa). Lanes 1 and 2 contain cell lysates from cells subject to oxidative stress. Lane 1 contains β-actin and γH2AX, while Lane 2 contains β-actin, adenoviral RAD51, and γH2AX. β- actin is used as a loading control antibody to ensure that protein loading is uniform across the lanes. β- actin expression was consistent in both lanes. Lane 2 had high RAD51 and low γH2AX expression; γH2AX expression is expected at a higher intensity than RAD51. RAD51 was expressed at 37-38 kDa, γH2AX at 15 kDa, and β-actin at 42 kDa.

It Should Be Noted that Bands Would Not Be Identical in a Real Western Blot. Bands were Made Identical for Illustrative Purposes, Allowing Readers to Focus on the Conceptual Understanding. [Graph Created by the Student Researcher Using Canva, 2024]

Max Score	Total Score	Query Cover	E. Value	Per. Ident	Acc. Len	Accession
1380	1380	100%	0.00	100.00%	9912	Query_606289

Figure 5: The BLAST (Basic Local Alignment Search Tool) Result showed that 100% of the query Sequence Was Identical to a Part of the Subject Sequence. The RAD51 Sequence Was Inserted as the Query, and the Experimental pAMHDAdGT8-4 sequence (FIGURE 2) was Inserted as the Subject. [Graph Created by the Student Researcher Using BLAST, 2024]

Methods (Note: The Experimental Design/Pre-Clinical Proposal is Carried out Both in Silico– SnapGene, BLAST–and in Proposed Laboratory Experiments.)

Cell Lines and Tissue Culture

The HEK 293T cell line used in the study would be obtained from Millipore Sigma. Cells would be derived from human fetal kidney cells. HEK 293T is an adherent cell line expressing the SV40 large T antigen. Therefore, this cell line is competent for replication of vectors with the SV40 signal.

The Human Lung Carcinoma Cell Line (A549) that was proposed in this study would be derived from the lung tissues of a 48-year-old Caucasian male with non-small cell lung cancer (NSCLC). A549 cells are ubiquitous in ROS-related studies and, therefore, make a suitable cell line for this study [32].

Restriction Enzyme Digestion Reaction

In silico, the digestion reaction involved cutting the lacZ gene at the KpNI and PspXI excision sites. The chosen plasmid for this study, plasmid pAMHDAdGT8-4 (addgene plasmid 26421), only had one specific excision site for each restriction enzyme (Figure 1). Digestion gave a clean cut, meaning that excision effectively separated the lacZ gene from the rest of the plasmid. Post-excision, the pAMHDAdGT8-4 plasmid was left with an open section for eventual insertion of the desired gene.

In a real lab, a combination of the following would be added to a microcentrifuge: 1 µg of adenoviral plasmid, 1x CutSmart buffer, 1µL of KpNI enzyme, 1µl of PspXI enzyme, and nuclease-free water to bring the total volume to 20 µl [2]. Then, the reaction would be incubated to excise the lacZ fragment sequence.

Gel Purification

In this study, electrophoresis was simulated via the SnapGene electrophoresis feature (Figure 3).

The built-in DNA ladder, lacZ gene, wild-type pAMHDAdGT8-4 sequence, and the digested pAMHDAdGT8-4 sequence were loaded into their respective in sillicolanes.

In a real laboratory, the 1% agarose gel would be prepared by mixing 1g agarose powder, 100 ml 1x TAE buffer, and 10 µl Syber Safe or EtBr [3]. After the solution solidifies, 5 µl DNA ladder, 200 ng of the lacZ gene, the wildtype pAMHDAdGT8-4 sequence, and the pAMHDAdGT8-4 digested fragments would be loaded into their respective lanes.

Gibson Assembly Method

In this study, the SnapGene Gibson Assembly feature was used to insert the RAD51-eGFP sequence into the space where the lacZ was before restriction enzyme digestion (Figure 1, Figure 2). With the exonuclease feature/simulation, the 5' overhangs were excised to create 3' single-stranded overhangs. We checked the RAD51-eGFP gene block sequence and the adenoviral backbone to ensure at least 25 bp of homology. The designed RAD51-eGFP fragment was inserted between the mCMV promoter and SV40 poly(A)tail signal (Figure 2).

In a laboratory, RAD51-eGFP fragments and the purified adenoviral backbone vector would be combined until they are in the range of 0.03-0.5 pmol and a ratio of 1:2 (insert: vector) [4]. Finally, the reaction would be incubated at 50°C for 60 minutes, yielding a continuous DNA molecule.

Bacterial Transformation

While this step was not simulated, it is a vital part of the experimental procedure. Bacterial transformation allows bacteria to incorporate foreign DNA genomes. In this process, after the Gibson mix is added to the Stellar cells, each colony growing after incubation in the ampicillin medium would indicate successful plasmid incorporation.

Inoculating a Bacterial Culture

In a real lab, a colony would be resuspended in 5 mL LB media containing 1x ampicillin antibiotic and grown for 14 hours at 37°C with 250 rpm shaking [5]. Transformation of the DNA is vital for the amplification of the DNA.

Miniprep to Prepare the Adenoviral Vector Plasmid

In a real laboratory, the plasmid amplified from the colony can be purified by Monarch® Plasmid
DNA Miniprep Kit (NEB #T1010). Bacterial cultures would be centrifuged, lysed, neutralized, and clarified before the supernatant is passed through a miniprep column, with purified plasmid DNA eluted in nuclease-free water. In a lab, Sanger sequencing would be completed to check whether the genetic insert in the adenoviral vector was correctly incorporated and matched the expected sequence. DNA fragments would then be separated based on size via capillary gel electrophoresis. As fragments exit the capillary tube, the fluorescent dyes are illuminated by a laser beam and detected by a photomultiplier.

Making Adenovirus in Human Embryonic Kidney 293 Cells (Hek 293t)

In this study, the BLAST sequencing showed that the simulated RAD51 insert's alignment was identical to its counterpart in the completed adenoviral vector (Figure 5). BLAST was done by inputting the RAD51 sequence and using the synthesized adenoviral vector as a reference. BLAST's localalignment algorithm and scoring matrices (BLOSUM62) were used to calculate how similar the two imputed sequences were.

In a laboratory, once the adenoviral vector sequence is confirmed, the design plasmid is transfected into HEK 293T cells, which are then split and counted to ensure 600,000 cells per well in a 6- well plate. Transfection occurs once the cells reach 60-80% confluency. After TransIT-LT1 Reagent and Opti-MEM addition, adenovirus production would be confirmed via flow cytometry [6].

Adenoviral Vector Transfection in Lung Carcinoma Cells (A549)

In a laboratory, the confirmed adenoviral vector plasmids would then be transfected into HEK 293T cells via cell splitting, transfection using TransIT-LT1 REagent, and adenovirus production confirmed by GFP fluorescence [6].

Flow Cytometry

Flow Cytometry is a technique used to analyze cell particles' physical and chemical characteristics as they flow in a stream through a laser light source. In this study, rather than GFP fluorescence, GFP prevalence is found in the SnapGene simulated versions of the genes.

In a lab, the complete adenoviral cells would be stained and passed through a nozzle surrounded by sheath fluid. The light that passes through the stained cells would be detected and quantified to measure the accuracy of adenoviral creation [7]. Thus, the successfully infected cells would result in a GFP-positive cell population. GFP expression in treated A549 cells would indicate successful infection, similar to its use in HEK 293T cells.

Oxidative Stress Induction in Cell Culture

Post-transfection A549 cells would be treated at 90% confluency with hydrogen peroxide to induce oxidative stress. The medium would then be aspirated, and the cells would be washed with PBS to remove residual hydrogen peroxide.

Western Blot

In this study, we created a Western Blot that assumes that all the previous steps went ideally (Figure 4). A western blot would measure the expression of RAD51 and γH2AX in the adenoviral cells (Figure 4). We analyzed the literature and found that, to some degree, RAD51 and γH2AX are inversely proportional. The lanes would be loaded according to Figure 4. Beta-actin (β-actin), a protein with a molecular weight of 42 kDa, is used as a reference marker to facilitate the clear differentiation and analysis of target proteins. In a lab, adenoviral cells would be lysed, homogenized, and centrifuged to extract proteins, which are prepared for SDS-PAGE. Proteins would be transferred to polyvinylidene fluoride (PVDF) membranes to enhance subsequent detection and quantification. PVDF membranes would be probed with appropriate primary antibodies and then incubated with anti-rabbit IgG and HRP-linked secondary antibodies [8].

Results (Note: The Results Presented Here Include Both in Silico Data (SnapGene, BLAST) and Expected Outcomes Based on Literature Review.)

The study aimed to design an adenoviral vector packaging RAD51 for pre-clinical tests to reduce ROS-induced DNA damage. Molecular cloning instruction for how to insert the RAD51 gene into the pAMHDAdGT8-4 adenoviral backbone was proposed. If future preclinical studies prove the efficacy of this proposed methodology, then RAD51 insertion would be a viable method to inhibit cancer progression in the TME.

The restriction digestion reaction effectively excised the lacZ gene from the pAMHDAdGT8-4 adenoviral backbone at 4505 bp (KpNI excision site) and 7666 bp (PspXI excision site), yielding two distinct fragments. Post-excision, electrophoresis confirmed precise cutting at the restriction sites (Figure 3). In Lane 1 of the gel, the uncut vehicle plasmid is around 3kb; the pAMHDAdGT8-4 adenoviral backbone may be running faster than its actual size due to supercoiling, which is characteristic of circular plasmids. In Lane 2, the lacZ gene fragment appears at 3 kb- 3.1 kb, which aligns with the expected size of lacZ. In Lane 3, the lane with the digested plasmid, there are two bands at around ~5 kb (the vector backbone) and ~3 kb (the lacZ fragment). In the gel, there is no indication of smearing or unexpected bands, meaning there was no partial digestion or degradation.

Gibson Assembly effectively ligated the RAD51-eGFP sequences into the space where the lacZ gene previously was (between the mCMV promoter and the SV40 poly(A) tail) (Figure 2). During incubation/simulation, exonucleases cleaved 3' single-strand overhangs to ensure effective annealing. After in silico single-strand resection, DNA polymerase fills in the gaps, and DNA ligase seals the nicks to ensure a continuous circular plasmid.

In a laboratory setting, bacterial transformation would introduce the recombinant plasmid DNA into Stellar E. coli cells to amplify the plasmids containing the RAD51 gene. Because vector backbones could contain an Ampicillin resistance gene (AmpR), an ampicillin medium would be necessary to ensure that grown bacteria have the adenvoiral-RAD51-eGFP while being ampicillin resistant (Figure 2).

In the lab, Sanger sequencing would be expected to verify the correct insertion of RAD51. Post- sequencing, BLAST tools aligned the sequencing result with the expected adenoviral sequence. and it was 100% identical–meaning no mismatches or mutations were found in the RAD51 gene sequence during the cloning process (Figure 5). In a lab, HEK 293T cells are expected to yield high levels of adenoviral particles. Subsequent infection of A549 cells would be measured with GFP expression, and assuming

accurate and efficient infection, there would be a high percentage of fluorescence.

In this simulation, as the genomes are fully visible (Figure 2), we do not need to check GFP fluorescence.
The results from the expected Western blot (Western Blot was assumed that all preceding steps were successful) indicate that when RAD51 levels are increased, the γH2AX concentration decreases (Figure 4). The γH2AX, which indicates an increase in DSBs, was highly expressed in the untreated lane, where the cell lysate would be exposed to oxidative stress without RAD51 supplementation. The γH2AX was less prominent in the treated lane, indicating that the addition of RAD51 resulted in a decrease in the number of DSBs. Furthermore, γH2AX was expected to have a higher intensity than RAD51 as it has a higher nTPM (transcripts per million) in A549 cells: γH2AX has 88.3 nTPM, whereas RAD51 only has 19.4 nTPM (data collected from Human Protein Atlas).

Discussion
Our in silico cloning simulation confirmed successful lacZ excision, seamless insertion of RAD51-eGFP, and 100% identity with BLAST algorithms. The preclinical analysis demonstrates that multiple steps in the RAD51 insertion process are feasible and effective–a novel gene therapy strategy to enhance DNA repair within the TME. Unlike conventional therapies that focus on introducing DNA damage (to kill metastatic tumor cells), our approach seeks to stabilize the genome of TME cells.

P53 is a tumor suppressor protein that plays a role in DNA repair, apoptosis, and cell cycle regulation. Prior studies have demonstrated the feasibility of inserting the p53 gene into adenoviral vectors [33]. In fact, various gene sequences, some longer and more complex than RAD51, have been successfully inserted into an adenoviral plasmid, reinforcing the viability of RAD51 insertion [31].

Furthermore, successful RAD51 insertion into cells in the TME could allow for localized repair and tumor control. A key aspect of tumor control is tumor growth inhibition and metastasis prevention [34]. RAD51 indirectly inhibits tumor growth and inadvertently prevents metastasis by strengthening the DNA of TME cells.

RAD51 can repair DSBs, and its efficacy can be measured with the γH2AX biomarker. Phosphorylated H2AX (γH2AX) increases analogously with DSBs [35]. At the damage site, γH2AX forms cohesion that holds DNA ends together, stabilizing the break and enabling repair [36]. Therefore, effective RAD51-mediated HR should correspond to fewer γH2AX foci, where high γH2AX foci levels suggest ineffective repair (Figure 4). If future studies demonstrate the viability of this gene therapy approach, then patients can reap many benefits. Researchers have demonstrated that tumors with stable genomes are less likely to develop resistance to treatments such as radiotherapy [37]. Radiotherapy induces free radicals via its high-energy radiation; when this radiation hits water molecules in the TME, ROS species are formed. An increased concentration of ROS may result in DSBs and further DNA damage.

By strengthening DNA with adenoviral vectors, the genomes of healthy cells in the TME will be less susceptible to ROS damage and more resistant to radiotherapy damage. In other words, patients will be able to withstand stronger radiotherapy treatments that do not risk a weakening TME genome. With stronger radiotherapy treatments, clinicians can more safely escalate radiation intensity–increasing the likelihood of tumor cell eradication. Furthermore, by stabilizing the genome, surrounding cells will be able to carry out their normal function without risk of mutation. Preventing mutations and stabilizing genomes will prevent metastasis and protect healthy cells.

CAFs are heavily influenced by the presence of DNA damage in the TME and are often located at the edge of tumors (close to the TME). When DNA damage is limited, there may be a slower rate of CAF proliferation, reducing the amount of chemokines, cytokines, and free radicals that can confer a pro- tumorigenic environment. With less genomic instability, RAD51 can stabilize the genome and counteract the effects of CAF, which may downregulate the TGF-β pathway and decrease fibroblast differentiation into CAFs [22]. With a lower concentration of CAFs, there may be limited tumor growth and metastasis.

Depending on the level of ROS in the TME before treatment, limiting the presence of CAFs could also reduce the overall ROS level. Typically, increased ROS results in CAV-1 downregulation [23]. If ROS is limited, then the activation of CAV-1 downregulation pathways will decrease–increasing CAV-1. Its downregulation results in stromal cells exhibiting a CAF phenotype (tumorigenic) [31]. When CAV-1 levels are brought closer to homeostatic levels, then fewer cells may exhibit the CAF phenotype, which could lead to a more stable TME with limited tumor progression.

Limitations
However, it must be noted that further research must be done before the clinical use of adenoviral vectors with RAD51. As the study was hypothesized based on SnapGene simulations, these results should be approached cautiously. An in silico study may not account for external confounding variables that may impede the results: the epidemiological heterogeneity Valde Iglesias et. al. highlighted will not be evinced in a simulation. Since the Western blot was assumed based on a simulation, the study does not include quantitative fold-change analysis or the traditional normalization techniques. Therefore, the Western Blot should be taken as a qualitative representation of simulated/theoretical findings.

Conclusion
After clinical validation, RAD51 insertion may serve as a possible treatment avenue for patients suffering from high-concentration ROS tumors. The simulated findings suggest that the generation of adenoviral vectors carrying RAD51 is viable. Furthermore, RAD51 insertion may pave the way for new gene therapy strategies that limit metastasis and prevent radiotherapy resistance. Currently, there is no adenoviral-based cancer treatment for solid tumors approved by the FDA, but the National Medical Products Administration (Chinese FDA equivalent) has approved adenovirus therapies that target solid tumors, like Gendicine and Oncrine. However, the FDA has approved adenoviral-based treatments for a specific type of in situ bladder carcinoma, nadofaragene firadenovec- vncg, but they have not approved a vector-based treatment for solid-state tumors. This paper aims to add to the growing body of evidence orroborating their therapeutic potential to hopefully support their integration into American medicine.

Nevertheless, in vivo studies are necessary to confirm these findings and study the long-term effects of RAD51 insertion. In vivo studies would help researchers more accurately understand the implications of RAD51 upregulation in the TME. Studies on long-term effects would demonstrate the durability of therapeutic effects and possible long-term consequences. With clinical data, the design and creation of the adenoviral plasmid can be improved (i.e. addition of enhancer elements near the SV40 sequence). If future clinical studies substantiate the simulated findings, then this work will have laid the foundation for a new paradigm in tumor

treatments that prioritizes genomic integrity over the traditional approach of inducing DNA damage.

References

1. Collin F (2019) Chemical Basis of Reactive Oxygen Species Reactivity and Involvement in Neurodegenerative Diseases. International journal of molecular sciences 20: 2407.
2. (2016) Restriction digest of plasmid DNA Addgene https://www.addgene.org/protocols/restriction-digest/ .
3. (2018) Create an agarose gel https://www.addgene.org/protocols/gel-electrophoresis/.
4. (2009) Gibson Assembly Cloning. Addgene https://www.addgene.org/protocols/gibson-assembly/.
5. (2017) Bacterial transformation. Addgene https://www.addgene.org/protocols/bacterial-transformation/.
6. (2015) AAV production in Hek293t cells Addgene https://pmc.ncbi.nlm.nih.gov/articles/PMC4817810/.
7. McKinnon KM (2018) Flow cytometry: An overview. Current protocols in immunology https://www.ncbi.nlm.nih.gov/pmc/articles/PMC5939936/.
8. (2022) Sample preparation for Western Blot. Abcam https://www.addgene.org/protocols/western-blot/.
9. Krylatov AV, Maslov LN, Voronkov NS, Boshchenko AA, Popov SV, et al. (2018) Reactive Oxygen Species as Intracellular Signaling Molecules in the Cardiovascular System. Current cardiology reviews 14: 290-300.
10. Zhou D, Shao L, Spitz DR (2014) Reactive oxygen species in normal and tumor stem cells. Advances in cancer research 122: 1-67.
11. (2019) NCI Dictionary of Cancer terms. Comprehensive Cancer Information - NCI. https://www.accc-cancer.org/home/learn/precision-medicine/cancer- diagnostics/biomarkers/biomarkerlive/lexicon/references.
12. Ferguson LR, Chen H, Collins AR., Connell M, Damia (2015) Genomic instability in human cancer: Molecular insights and opportunities for therapeutic attack and prevention through diet and nutrition. Seminars in cancer biology 35: 5-24.
13. Liberti MV, Locasale JW (2016) The Warburg Effect: How Does it Benefit Cancer Cells? Trends in biochemical sciences 41: 211-218.
14. Bhutta BS (2024) Hypoxia. Stat Pearls. https://www.ncbi.nlm.nih.gov/books/ NBK482316/
15. David SS, O'Shea VL, Kundu S (2007) Base-excision repair of oxidative DNA damage. Nature 447: 941-950.
16. Aller P, Rould MA, Hogg M, Wallace SS, Doublié S (2007) A structural rationale for stalling of a replicative DNA polymerase at the most common oxidative thymine lesion, thymine glycol. Proceedings of the National Academy of Sciences of the United States of America 104: 814-818.
17. Dolinnaya NG, Kubareva EA, Romanova EA, Trikin RM, Oretskaya TS (2013) Thymidine glycol: the effect on DNA molecular structure and enzymatic processing. Biochimie 95: 134-147.
18. Glabman RA, Choyke PL, Sato N (2022) Cancer-Associated Fibroblasts: Tumorigenicity and Targeting for Cancer Therapy. Cancers 14: 3906.
19. Chung J, Huda MN, Shin Y, Han S, Akter S, et al. (2021) Correlation between Oxidative Stress and Transforming Growth Factor-Beta in Cancers. International journal of molecular sciences 22: 13181.
20. Weinberg F, Ramnath N, Nagrath D (2019) Reactive Oxygen Species in the Tumor Microenvironment: An Overview. Cancers 11: 1191.
21. Chen D, Che G (2014) Value of caveolin-1 in cancer progression and prognosis: Emphasis on cancer-associated fibroblasts, human cancer cells and mechanism of caveolin-1 expression (Review). Oncology letters 8: 1409-1421.
22. Glabman RA, Choyke PL, Sato N (2022) Cancer-Associated Fibroblasts: Tumorigenicity and Targeting for Cancer Therapy. Cancers 14: 3906.
23. Martinez Outschoorn UE, Balliet RM, Rivadeneira DB, Chiavarina B, Pavlides S, et al. (2010) Oxidative stress in cancer associated fibroblasts drives tumor-stroma co-evolution: A new paradigm for understanding tumor metabolism, the field effect and genomic instability in cancer cells. Cell cycle (Georgetown, Tex.) 9: 3256-3276.
24. Weng MS, Chang JH, Hung WY, Yang YC, Chien MH (2018) The interplay of reactive oxygen species and the epidermal growth factor receptor in tumor progression and drug resistance. Journal of experimental & clinical cancer research: CR 37: 61.
25. Shintani Y, Kimura T, Funaki S, Ose N, Kanou T, et al. (2023) Therapeutic Targeting of Cancer-Associated Fibroblasts in the Non-Small Cell Lung Cancer Tumor Microenvironment. Cancers 15: 335.
26. Zhu J, Wang S, Yang D, Xu W, Qian H (2023) Extracellular vesicles: emerging roles, biomarkers and therapeutic strategies in fibrotic diseases. Journal of nanobiotechnology 21: 164.
27. Paggetti J, Haderk F, Seiffert M, Janji B, Distler U, et al. (2015) Exosomes released by chronic lymphocytic leukemia cells induce the transition of stromal cells into cancer-associated fibroblasts. Blood 126: 1106-1117.
28. Carrà G, Ermondi G, Riganti C, Righi L, Caron G, et al. (2021) IκBα targeting promotes oxidative stress-dependent cell death. Journal of experimental & clinical cancer research: CR 40: 136.
29. Roth JA (2006) Adenovirus p53 gene therapy. Expert opinion on biological therapy 6: 55-61.
30. Cook KM, Figg WD (2010) Angiogenesis inhibitors: current strategies and future prospects.
31. CA: a cancer journal for clinicians 60: 222-243.
32. Pinto DM, Flaus A (2010) Structure and function of histone H2AX. Sub-cellular biochemistry 50: 55-78.
33. (2012) Histone H2AX. Histone H2AX - an overview | ScienceDirect Topics (n.d.) https://pmc.ncbi.nlm.nih.gov/articles/PMC3371125/.
34. Nickoloff JA, Taylor L, Sharma N, Kato TA (2021) Exploiting DNA repair pathways for tumor sensitization, mitigation of resistance, and normal tissue protection in radiotherapy. Cancer drug resistance (Alhambra, Calif.) 4: 244-263.
35. Zheng Z, Su J, Bao X, Wang H, Bian C, et al. (2023) Mechanisms and applications of radiation-induced oxidative stress in regulating cancer immunotherapy. Frontiers in immunology 14: 1247268.
36. (2020) Ionization and cell damage. Nondestructive Evaluation NDE Engineering: Radiation Safety. (n.d.) https://ntrs.nasa.gov/api/citations/20200002023/downloads/20200002023.pdf.
37. Valdiglesias V, Giunta S, Fenech M, Neri M, Bonassi S (2013) γH2AX as a marker of DNA double strand breaks and genomic instability in human population studies. Mutation research 753: 24-40.
38. Colbert L, Jia Y, Sharma A, Hu J, Xu Z, et al. (2025) FDA Approval Summary: Nadofaragene Firadenovec-vncg for Bacillus Calmette-Guérin-Unresponsive Non-Muscle-Invasive Bladder Cancer. Clin Cancer Res 31: 1182-1185.